2011 American Control Conference
on O'Farrell Street, San Francisco, CA, USA
June 29 - July 01, 2011

A Direct Adaptive Method for Discriminating Sinusoidal Components with Nearby Frequencies

Gilberto Pin and Thomas Parisini

Abstract— **This paper deals with the on-line simultaneous estimation of frequencies, amplitudes, and phases of a pair of sinusoidal signals with values of the frequencies that are close to each other. The proposed nonlinear parametric identification method is based on the interconnection of two quadrature-based adaptive filters, originally conceived for the extraction of a single sinusoidal signal. The distinctive feature of quadrature-based filters, inherited by the method under consideration, consists in performing the adaptation in a parametric space having higher dimensions than the number of unknowns. The stability analysis, based on two-time scale averaging arguments, shows the existence of multiple asymptotically stable manifolds corresponding to the simultaneous detection of the two sinusoidal signals.**

I. Introduction

The problem of estimating the characteristic parameters of multiple sinusoids with unknown frequencies, phases and amplitudes has received considerable attention of researchers in the field of signal processing (see [1], [2], [3], [4] and the references therein), multi-tonal sound extraction and noise attenuation (see [5], [6] and [7]), power system's monitoring ([8], [9]), vibration suppression and control, etc..

Typically, the problem of detecting multiple sinusoids is approached by means of the Fourier Transform, associated to some peak detection heuristics, based on energy consideration (see [1], [2], [3]). For the practical implementation of the method, the signal is sampled in time with a suitably small sampling period and then arrays of data are collected for further batch elaboration. Although this technique is particularly suited for the real-time implementation (thanks to the efficiency of Fast Fourier Transform (FFT) algorithms), it also presents some drawbacks: the maximum dimension of the batch window limits from above the minimum frequency which can be accounted for by the method, while the sampling interval introduced quantization in the frequency domain, that is, the resolution of the frequency estimator is affected by the sampling rate.

To overcome the quantization issue of the FFT, it has been suggested by many authors to use a bank of single-sinusoid estimators, each one in charge of detecting frequency, phase and amplitude of a single component. Moreover, in many cases, the complexity of these filters is even lower than that of FFT. Among the various methods for frequency detection proposed in the literature, the Kalman Filter, [10], and the Extended Kalman Filter (EKF) have attracted increasing interest among practitioners (see, e.g., [11]), both for the strong theoretical basis and the ease of implementation. Nonetheless, both the the EKF is known to be very sensitive with respect to its tuning parameters. In this regard, Adaptive Notch Filtering (ANF) represents a valid alternative when an accurate model of the process is not available (see [12], [13] and [14]). This technique consists of a very sharp notch whose base frequency adaptively tracks that of the input signal.

A major issue in multiple-frequency identification with a bank of adaptive filters in parallel is that it is possible for two or more estimators to converge to the same frequency value, leaving some component of the signal unaccounted for. One of the most used techniques to overcome this issue is the cascaded ANF (see [5] anf [15]), which has superior performance compared to FFT in terms of computational efficiency and convergence rate (it can be used in hardware with limited computational resources, too). The cascade ANF is composed of p notch filters of order 2 in series to estimate p frequencies of p sinusoids. Each notch filter undergoes an on-line adaptation to minimize the time-averaged norm of the residual signal. It is worth noting that this architecture works in practice only when the sinusoids can be sorted hierarchically according to their amplitudes, such that the 1-st filter cancels the fundamental harmonic and so on. Even after the full convergence, the frequency estimates of a cascaded ANF do not perfectly settle upon fixed values, but oscillations are observed in particular in the higher-order modules. The presence of such limit cycles, known as the "beating phenomena", is due to the mutual interaction between the estimators. Only by using some a priori informations, such that the sinusoids are harmonically related, and which order harmonics are dominant, it is possible to mitigate the beating effect by applying ad-hoc techniques based on heuristic arguments.

An alternative to the cascaded ANF has been proposed by Guo and Bodson [16] for the two-sinusoidal signals case. It is based on a supervisory discrete-time logic which detects those pathological situations in which the two filters converge to the same frequency, thus forcing the separation of the two estimates.

In this framework, we are going to describe a technique capable to extract the characteristic parameters of a couple of sinusoidal signals from their sum-signal in real-time, avoiding, at the same time, the beating phenomenon. The proposed method, compared to [16], relies on the continuous-time dynamic decoupling of two nonlinear quadrature-based frequency-adaptive filters (FAF), operated by a so-called de-correlator block, while a supervisory logic is only provided to detect the single-sinusoid case. The architecture of the multiple-frequency estimation scheme is depicted in Figure 1, that will be explained later on. The use of nonlinear quadrature-based filters is motivated by the robustness shown by these estimators in facing the presence of both noise and time-varying fundamental frequencies (see [17] and the references therein). Moreover, the stability properties of the

G. Pin is with Danieli Automation S.p.A, Udine, Italy (g.pin@dca.it); T. Parisini is with the Dept. of Electrical and Electronic Engineering at the Imperial College London, UK and also with the Dept. of Industrial and Information Engineering at the University of Trieste, Italy (t.parisini@paperplaza.net)

978-1-4577-0079-8/11/$26.00 ©2011 AACC

overall dynamical system emerging from the interconnection of the nonlinear quadrature-based estimators can be analyzed toward the equilibria by means of nonlinear averaging methods, such that it is possible to characterize the effect of the tuning parameters on the convergence of the estimator.

The paper is organized as follows: In Section II, the problem of two sinusoidal terms detection will be formalize and the architecture of the estimator will be introduced. In Section III, the stability properties of the filter will be analyzed by means of a two-time scale averaging analysis. Finally, in Section IV the effectiveness of the proposed scheme will be shown through a simulation example.

II. Two-sinusoid detection by the interconnection of quadrature-based filters

Let us consider the following signal, consisting in the sum of two sinusoids having unknown, but time-invariant, amplitudes $(A_1,\, A_2)$, frequencies $(\omega_1,\, \omega_2)$ and phases $(\vartheta_1,\, \vartheta_2)$:

$$v(t) \;=\; A_1 \sin(\omega_1 t + \vartheta_1) + A_2 \sin(\omega_2 t + \vartheta_2). \tag{1}$$

The signal $v(t)$ can be equivalently expressed as:

$$\begin{aligned} v(t) \;=\; & a_1 \sin(\omega_1 t + \phi_1) + c_1 \cos(\omega_1 t + \phi_1) + \\ & a_2 \sin(\omega_2 t + \phi_2) + c_2 \cos(\omega_2 t + \phi_2), \end{aligned} \tag{2}$$

where the parameters a_i, c_i and ϕ_i, $i \in \{1, 2\}$ verify $A_i \triangleq \sqrt{a_i^2 + c_i^2}$ and $\phi_i = \vartheta_i + \delta_i$, being

$$\delta_i = \operatorname{acos}\left(\frac{a_i}{A_i}\right) \operatorname{sign}(c_i) \tag{3}$$

the phase lag between each of the sinusoids in (1) and the sinusoidal component of the quadrature (Fourier) representation (2). Note that for each sinusoid $A_i \sin(\omega_i t + \vartheta_i)$, $i \in \{1, 2\}$, there are ∞ quadruplets $(a_i, c_i, \phi_i, \omega_i)$ in the quadrature representation which verify the identity (1).

In the work [18], it has been shown that, for the single-sinusoid detection case, it is possible to estimate the triplet $(A, \omega, \vartheta) \in \mathbb{R}^3$ by performing the adaptation in the higher dimensional parameter space of the quadruplets $(a, c, \phi, \omega) \in \mathbb{R}^4$ by means of a Frequency-Adaptive quadrature-based Filter (FAF). In particular, the existence of a manifold $\Omega \in \mathbb{R}^4$ containing asymptotically stable equilibria in the extended parametric space has been proven, ensuring the local stability of the filter. Moreover, a direct correspondence has been established between the characteristic parameters of the estimator and its convergence speed.

Next, we will consider the problem of detecting two sinusoidal signals with different frequencies $(\omega_1 \neq \omega_2)$, for which $A_1 > 0$ and $A_2 > 0$.

Relying on the interconnection of a couple of frequency-adaptive quadrature-based filters (denoted as FAF_A and FAF_B) and on a decorrelator (see Figure 1), the proposed method allows the complete detection of the two distinct sinusoidal components. Considering the underlying architecture as a single parametric identification scheme for the six unknowns $(A_1, \omega_1, \vartheta_1, A_2, \omega_2, \vartheta_2) \in \mathbb{R}^6$, then the proposed method inherits from the FAF the property of performing the adaptation in a higher dimensional parametric space. In this case the adaptation involves 10 variables: the 10-plet $(\hat{a}_A, \hat{c}_A, \hat{\phi}_A, \hat{\omega}_A, \hat{a}_B, \hat{c}_B, \hat{\phi}_B, \hat{\omega}_B, \hat{a}_C, \hat{c}_C) \in \mathbb{R}^{10}$ is expected to converge to any of the admissible 10-plets $(a_A, c_A, \phi_A, \omega_A, a_B, c_B, \phi_B, \omega_B, a_C, c_C)$ belonging to the following manifolds:

$$\Omega_{A,1,B,2} \triangleq \left\{ \begin{array}{l} (a_A, c_A, \phi_A, \omega_A, a_B, c_B, \phi_B, \omega_B, a_C, c_C) \in \mathbb{R}^{10}: \\ \omega_A = \omega_1,\, \sqrt{a_A^2 + c_A^2} = A_1,\, \phi_A + \delta_A = \vartheta_1, \\ \omega_B = \omega_2,\, \sqrt{a_B^2 + c_B^2} = A_2,\, \phi_B + \delta_B = \vartheta_2, \\ a_C = 0, c_C = 0; \end{array} \right\}$$

$$\Omega_{A,2,B,1} \triangleq \left\{ \begin{array}{l} (a_A, c_A, \phi_A, \omega_A, a_B, c_B, \phi_B, \omega_B, a_C, c_C) \in \mathbb{R}^{10}: \\ \omega_A = \omega_2,\, \sqrt{a_A^2 + c_A^2} = A_2,\, \phi_A + \delta_A = \vartheta_2, \\ \omega_B = \omega_1,\, \sqrt{a_B^2 + c_B^2} = A_1,\, \phi_B + \delta_B = \vartheta_1, \\ a_C = 0, c_C = 0; \end{array} \right\}$$

which correspond to the case of complete discrimination/detection of the two sinusoidal terms. In particular, while the two FAFs (FAF_A and FAF_B) are associated to the first eight parameters, the variables $\hat{a}_C$ and $\hat{c}_C$ belong to the decorrelator module, which is responsible for "steering" the two FAFs to different frequencies. Next, the differential equations governing the devised detection scheme will be introduced and discussed.

As far as Figure 1 is concerned, letting $\hat{v}_A(t)$, $\hat{v}_B(t)$ and $\hat{v}_C(t)$ be defined as

$$\begin{aligned} \hat{v}_A(t) &\triangleq \hat{a}_A(t) \sin(\hat{\theta}_A(t)) + \hat{c}_A(t) \cos(\hat{\theta}_A(t)) \\ \hat{v}_B(t) &\triangleq \hat{a}_B(t) \sin(\hat{\theta}_B(t)) + \hat{c}_B(t) \cos(\hat{\theta}_B(t)) \\ \hat{v}_C(t) &\triangleq \hat{a}_C(t) \sin(\hat{\theta}_C(t)) + \hat{c}_C(t) \cos(\hat{\theta}_C(t)) \end{aligned}$$

and considering the interconnections among the quadrature-based filters and the decorrelator, the following adaptation laws for the parameters of FAF_A are proposed:

$$\left\{ \begin{array}{l} \dot{\hat{a}}_A(t) = \lambda \Big[\sin\Big(\hat{\theta}_A(t)\Big)\, v(t) - \sin\Big(\hat{\theta}_A(t)\Big) \times \\ \qquad\qquad \Big(\hat{v}_A(t) + \hat{v}_B(t) + \mu_C \hat{v}_C(t)\Big) \Big] \\ \dot{\hat{c}}_A(t) = \lambda \Big[\cos\Big(\hat{\theta}_A(t)\Big)\, v(t) - \cos\Big(\hat{\theta}_A(t)\Big) \times \\ \qquad\qquad \Big(\hat{v}_A(t) + \hat{v}_B(t) + \mu_C \hat{v}_C(t)\Big) \Big] \\ \dot{\hat{\theta}}_A(t) = \quad \mu_\theta \dot{\hat{\delta}}_A(t) + \hat{\omega}_A(t) \\ \dot{\hat{\omega}}_A(t) = \quad \mu_\omega \dot{\hat{\delta}}_A(t) \end{array} \right. \tag{4}$$

while the parameters of FAF_B evolve according to

$$\left\{ \begin{array}{l} \dot{\hat{a}}_B(t) = \lambda \Big[\sin\Big(\hat{\theta}_B(t)\Big)\, v(t) - \sin\Big(\hat{\theta}_B(t)\Big) \times \\ \qquad\qquad \Big(\hat{v}_A(t) + \hat{v}_B(t) - \mu_C \hat{v}_C(t)\Big) \Big] \\ \dot{\hat{c}}_B(t) = \lambda \Big[\cos\Big(\hat{\theta}_B(t)\Big)\, v(t) - \cos\Big(\hat{\theta}_B(t)\Big) \times \\ \qquad\qquad \Big(\hat{v}_A(t) + \hat{v}_B(t) - \mu_C \hat{v}_C(t)\Big) \Big] \\ \dot{\hat{\theta}}_B(t) = \quad \mu_\theta \dot{\hat{\delta}}_B(t) + \hat{\omega}_B(t) \\ \dot{\hat{\omega}}_B(t) = \quad \mu_\omega \dot{\hat{\delta}}_B(t) \end{array} \right. \tag{5}$$

where $\lambda \in \mathbb{R}_{>0}$, $\mu_\theta \in \mathbb{R}_{>0}$, $\mu_\omega \in \mathbb{R}_{>0}$ and $\mu_C \in \mathbb{R}_{>0}$ are tuning parameters.

The intuition behind the derivation of the filter consists in that, if FAF_A and FAF_B are initialized the same way, then they both start to track the fundamental frequency with the same adaptation transient. Then, the decorrelator starts to extract from the output of FAF_B the component in synchronous with FAF_A, re-injecting the signal with opposite sign at the two inputs of the FAFs, which therefore are fed with different signals.

In view of (3), the time-derivative of the phase lags

Fig. 1 Architecture of the two-frequency detection method, consisting of two frequency-adaptive quadrature-based filters (FAF_A and FAF_B) with a decorrelation module. The Decorrelator_C is responsible for "steering" the two estimated frequencies toward different values.

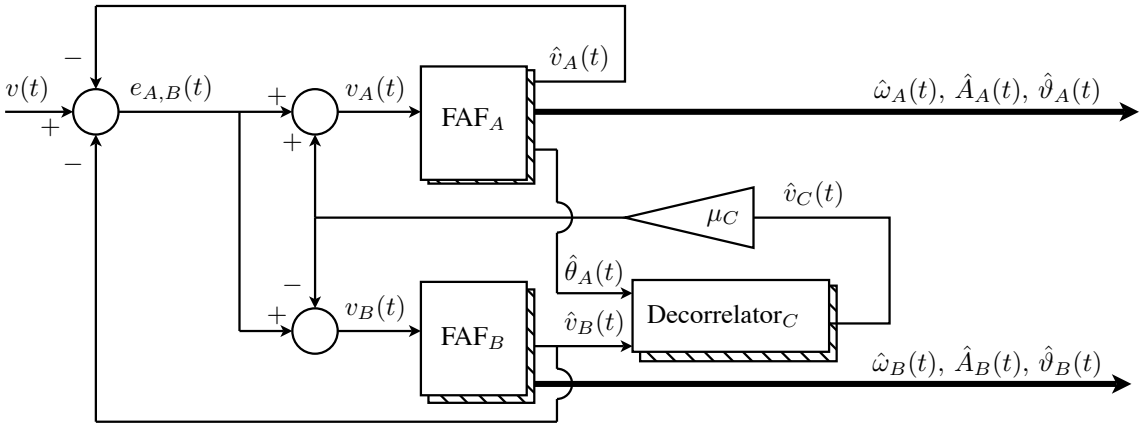

$\hat{\delta}_i(t), i \in \{A, B\}$ is given by

$$\dot{\hat{\delta}}_i(t) = \dot{\hat{\delta}}_i\left(\hat{a}_i(t), \hat{c}_i(t)\right) = -\left(\frac{\hat{c}_i(t)}{\hat{A}_i^2(t)}\dot{\hat{a}}_i(t) - \frac{\hat{a}_i(t)}{\hat{A}_i^2(t)}\dot{\hat{c}}_i(t)\right). \tag{6}$$

Finally, the dynamics of the decorrelator is described by

$$\begin{cases} \dot{\hat{a}}_C(t) = \lambda \sin\left(\hat{\theta}_C(t)\right)\left(\hat{v}_B(t) - \hat{v}_C(t)\right) \\ \dot{\hat{c}}_C(t) = \lambda \cos\left(\hat{\theta}_C(t)\right)\left(\hat{v}_B(t) - \hat{v}_C(t)\right). \end{cases} \tag{7}$$

Note that the decorrelator inherits the instantaneous phase from the FAF_A (that is, $\hat{\theta}_C(t) = \hat{\theta}_A(t)$). The phase inheritance also implies that the signal generated by the decorrelator has fundamental frequency $\hat{\omega}_C(t) = \hat{\omega}_A(t)$, when $\dot{\hat{a}}_C(t) = 0$ and $\dot{\hat{c}}_C(t) = 0$.

By performing a stability analysis based on averaging, we will show that the manifolds $\Omega_{A,1,B,2}$ and $\Omega_{A,2,B,1}$ contain stable equilibria for the estimator.

III. Stability analysis

Given the true parameters of the sinusoidal terms, namely $A_1, \omega_1, \vartheta_2$ and $A_2, \omega_2, \vartheta_1$, let us consider an admissible target 10-plet $(a_A, c_A, \phi_A, \omega_A, a_B, c_B, \phi_B, \omega_B, 0, 0) \in \Omega_{A,1,B,2}$. Let us introduce the error variables $\tilde{a}_A(t) \triangleq \hat{a}_A(t) - a_1$, $\tilde{a}_B(t) \triangleq \hat{a}_B(t) - a_2$,$\tilde{c}_A(t) \triangleq \hat{c}_A(t) - c_1$, $\tilde{c}_B(t) \triangleq \hat{c}_B(t) - c_2$, $\tilde{\omega}_A(t) \triangleq \hat{\omega}_A(t) - \omega_1$, $\tilde{\omega}_B(t) \triangleq \hat{\omega}_B(t) - \omega_2$, $\tilde{\phi}_A(t) \triangleq \hat{\phi}_A(t) - \phi_1$, $\tilde{\phi}_B(t) \triangleq \hat{\phi}_B(t) - \phi_2$, $\tilde{\psi}_A(t) \triangleq -(\tilde{\phi}_1 + \tilde{\omega}_1 t) = \omega_1 t + \phi_1 - \hat{\theta}_A(t)$, $\tilde{\psi}_B(t) \triangleq -(\tilde{\phi}_2 + \tilde{\omega}_2 t) = \omega_2 t + \phi_2 - \hat{\theta}_B(t)$ and let us set $\tilde{a}_C(t) = \hat{a}_C(t)$, $\tilde{c}_C(t) = \hat{c}_C(t)$. From

$$\begin{aligned} v(t) =& a_1 \sin\left(\hat{\theta}_A(t) + \tilde{\psi}_A(t)\right) + c_1 \cos\left(\hat{\theta}_A(t) + \tilde{\psi}_A(t)\right) \\ &+ a_2 \sin\left(\hat{\theta}_B(t) + \tilde{\psi}_B(t)\right) + c_2 \cos\left(\hat{\theta}_B(t) + \tilde{\psi}_B(t)\right) \\ =& a_1 \sin\left(\hat{\theta}_A(t)\right)\cos\left(\tilde{\psi}_A(t)\right) + a_1 \cos\left(\hat{\theta}_A(t)\right)\sin\left(\tilde{\psi}_A(t)\right) \\ &+ c_1 \cos\left(\hat{\theta}_A(t)\right)\cos\left(\tilde{\psi}_A(t)\right) - c_1 \sin\left(\hat{\theta}_A(t)\right)\sin\left(\tilde{\psi}_A(t)\right) \\ &+ a_2 \sin\left(\hat{\theta}_B(t)\right)\cos\left(\tilde{\psi}_B(t)\right) + a_2 \cos\left(\hat{\theta}_B(t)\right)\sin\left(\tilde{\psi}_B(t)\right) \\ &+ c_2 \cos\left(\hat{\theta}_B(t)\right)\cos\left(\tilde{\psi}_B(t)\right) - c_2 \sin\left(\hat{\theta}_B(t)\right)\sin\left(\tilde{\psi}_B(t)\right) \end{aligned} \tag{8}$$

it follows that the error dynamics for the overall system can be expressed as

$$\begin{aligned} \dot{\tilde{a}}_A(t) =& \lambda \sin\left(\hat{\theta}_A(t)\right)\Big\{ -\tilde{a}_A(t)\sin\left(\hat{\theta}_A(t)\right) - \tilde{c}_A(t)\cos\left(\hat{\theta}_A(t)\right) \\ &+ \mu_C\, \tilde{a}_C(t)\sin\left(\hat{\theta}_A(t)\right) + \mu_C\, \tilde{c}_C(t)\cos\left(\hat{\theta}_A(t)\right) \\ &+ a_1 \sin\left(\hat{\theta}_A(t)\right)\left[\cos\left(\tilde{\psi}_A(t)\right) - 1\right] + a_1 \cos\left(\hat{\theta}_A(t)\right)\sin\left(\tilde{\psi}_A(t)\right) \\ &+ c_1 \cos\left(\hat{\theta}_A(t)\right)\left[\cos\left(\tilde{\psi}_A(t)\right) - 1\right] - c_1 \sin\left(\hat{\theta}_A(t)\right)\sin\left(\tilde{\psi}_A(t)\right) \\ &- \tilde{a}_B(t)\sin\left(\hat{\theta}_B(t)\right) - \tilde{c}_B(t)\cos\left(\hat{\theta}_B(t)\right) \\ &+ a_2 \sin\left(\hat{\theta}_B(t)\right)\left[\cos\left(\tilde{\psi}_B(t)\right) - 1\right] + a_B \cos\left(\hat{\theta}_B(t)\right)\sin\left(\tilde{\psi}_B(t)\right) \\ &+ c_2 \cos\left(\hat{\theta}_B(t)\right)\left[\cos\left(\tilde{\psi}_B(t)\right) - 1\right] - c_2 \sin\left(\hat{\theta}_B(t)\right)\sin\left(\tilde{\psi}_B(t)\right)\Big\} \\ \dot{\tilde{c}}_A(t) =& \lambda \cos\left(\hat{\theta}_A(t)\right)\Big\{ \ldots \Big\} \\ \dot{\tilde{\psi}}_A(t) =& -\tilde{\omega}_A(t) - \mu_\theta \dot{\hat{\delta}}_A(t) \\ \dot{\tilde{\omega}}_A(t) =& \mu_\omega \dot{\hat{\delta}}_A(t) \end{aligned}$$

$$
\begin{aligned}
\dot{\tilde{a}}_B(t)=&\lambda\sin\Big(\hat{\theta}_B(t)\Big)\Big\{-\tilde{a}_A(t)\sin\Big(\hat{\theta}_A(t)\Big)-\tilde{c}_A(t)\cos\Big(\hat{\theta}_A(t)\Big)\\
&-\mu_c\,\tilde{a}_C(t)\sin\Big(\hat{\theta}_A(t)\Big)-\mu_C\,\tilde{c}_C(t)\cos\Big(\hat{\theta}_A(t)\Big)\\
&+a_1\sin\Big(\hat{\theta}_A(t)\Big)\Big[\cos\Big(\tilde{\psi}_A(t)\Big)-1\Big]+a_1\cos\Big(\hat{\theta}_A(t)\Big)\sin\Big(\tilde{\psi}_A(t)\Big)\\
&+c_1\cos\Big(\hat{\theta}_A(t)\Big)\Big[\cos\Big(\tilde{\psi}_A(t)\Big)-1\Big]-c_1\sin\Big(\hat{\theta}_A(t)\Big)\sin\Big(\tilde{\psi}_A(t)\Big)\\
&-\tilde{a}_B(t)\sin\Big(\hat{\theta}_B(t)\Big)-\tilde{c}_B(t)\cos\Big(\hat{\theta}_B(t)\Big)\\
&+a_2\sin\Big(\hat{\theta}_B(t)\Big)\Big[\cos\Big(\tilde{\psi}_B(t)\Big)-1\Big]+a_2\cos\Big(\hat{\theta}_B(t)\Big)\sin\Big(\tilde{\psi}_B(t)\Big)\\
&+c_2\cos\Big(\hat{\theta}_B(t)\Big)\Big[\cos\Big(\tilde{\psi}_B(t)\Big)-1\Big]-c_2\sin\Big(\hat{\theta}_B(t)\Big)\sin\Big(\tilde{\psi}_B(t)\Big)\Big\}\\
\dot{\tilde{c}}_B(t)=&\lambda\cos\Big(\hat{\theta}_B(t)\Big)\Big\{...\Big\}\\
\dot{\tilde{\psi}}_B(t)=&-\tilde{\omega}_B(t)-\mu_\theta\dot{\hat{\delta}}_B(t)\\
\dot{\tilde{\omega}}_B(t)=&\,\mu_\omega\dot{\hat{\delta}}_B(t)\\
\dot{\tilde{a}}_C(t)=&\lambda\sin\Big(\hat{\theta}_A(t)\Big)\Big\{-\tilde{a}_B(t)\sin\Big(\hat{\theta}_B(t)\Big)-\tilde{c}_B(t)\cos\Big(\hat{\theta}_B(t)\Big)\\
&+a_2\sin\Big(\hat{\theta}_B(t)\Big)\Big[\cos\Big(\tilde{\psi}_B(t)\Big)-1\Big]+a_2\cos\Big(\hat{\theta}_B(t)\Big)\sin\Big(\tilde{\psi}_B(t)\Big)\\
&+c_2\cos\Big(\hat{\theta}_B(t)\Big)\Big[\cos\Big(\tilde{\psi}_B(t)\Big)-1\Big]-c_2\sin\Big(\hat{\theta}_B(t)\Big)\sin\Big(\tilde{\psi}_B(t)\Big)\\
&-\tilde{a}_C(t)\sin(\hat{\theta}_A(t))-\tilde{c}_C(t)\cos(\hat{\theta}_A(t))\Big\}\\
\dot{\tilde{c}}_C(t)=&\lambda\cos\Big(\hat{\theta}_A(t)\Big)\Big\{-\tilde{a}_B(t)\sin\Big(\hat{\theta}_B(t)\Big)-\tilde{c}_B(t)\cos\Big(\hat{\theta}_B(t)\Big)\\
&+a_2\sin\Big(\hat{\theta}_B(t)\Big)\Big[\cos\Big(\tilde{\psi}_B(t)\Big)-1\Big]+a_2\cos\Big(\hat{\theta}_B(t)\Big)\sin\Big(\tilde{\psi}_B(t)\Big)\\
&+c_2\cos\Big(\hat{\theta}_B(t)\Big)\Big[\cos\Big(\tilde{\psi}_B(t)\Big)-1\Big]-c_2\sin\Big(\hat{\theta}_B(t)\Big)\sin\Big(\tilde{\psi}_B(t)\Big)\\
&-\tilde{a}_C(t)\sin(\hat{\theta}_A(t))-\tilde{c}_C(t)\cos(\hat{\theta}_A(t))\Big\}
\end{aligned}
\tag{9}
$$

with $\hat{\theta}_A(t)=\omega_1 t+\phi_1-\tilde{\psi}_A(t)$, $\hat{\theta}_B(t)=\omega_2 t+\phi_2-\tilde{\psi}_B(t)$ and where the bracketed expressions $\{...\}$ in the 2-nd and 6-th differential equations have been used to compact the notation.

Now, a two-time scale averaging analysis can be performed to analyze the behavior of the estimator. Given a time-variant differential system in the form

$$\dot{x}(t)=\lambda f(t,x(t)),\ x(0)=x_0, \tag{10}$$

the averaging analysis relates the properties of the solutions of (10) to the solutions of the so-called "averaged" system

$$\dot{\overline{x}}(t)=\lambda\overline{f}(\overline{x}(t)),\ \overline{x}(0)=x_0, \tag{11}$$

$$\overline{f}(z)\triangleq\lim_{T\to\infty}\frac{1}{T}\int_0^T f(\tau,z)\,d\tau. \tag{12}$$

As widely discussed in literature (see e.g., [19], [20] and [21]), the stability properties of the original system, for small values of λ, can be inferred from those of the averaged counterpart. However, since in our setup the phases $\hat{\theta}_A(t)$ and $\hat{\theta}_B(t)$ undergo an on-line adaptation, they do not evolve linearly in time, and their trends depend on the particular initial frequency estimation error. The stability analysis in this situation can be performed by advocating two-time scale averaging arguments. Indeed, considering the dynamics of $\tilde{\psi}_A(t)$ and $\tilde{\psi}_B(t)$, we can write

$$\hat{\theta}_A(t)=\omega_1 t+\phi_1+\tilde{\psi}_A(0)-\int_0^t\Big(\tilde{\omega}_A(\tau)+\mu_\theta\dot{\hat{\delta}}_A\Big)\,d\tau$$

$$\hat{\theta}_B(t)=\omega_2 t+\phi_2+\tilde{\psi}_B(0)-\int_0^t\Big(\tilde{\omega}_B(\tau)+\mu_\theta\dot{\hat{\delta}}_B\Big)\,d\tau$$

For a suitably small value of λ, it is possible to take $\dot{\hat{\delta}}_A\approx 0$ and $\tilde{\omega}_A(\tau)$ frozen to the initial value, that is $\tilde{\omega}_A(\tau)\approx\tilde{\omega}_A(0),\forall\tau\in[0,+\infty]$. Nonetheless, these positions (which hold as approximations for arbitrary initial conditions) are exact in correspondence of the equilibria, and thus they can be exploited to analyze the local stability properties of the averaged system. Under the two-time scales separation assumption, we will make use of the following approximations:

$$
\begin{aligned}
\hat{\theta}_A(t)&\approx(\omega_1-\tilde{\omega}_A(0))t+\phi_1+\tilde{\psi}_A(0)\\
&=\hat{\omega}_A(0)\,t+\phi_1+\tilde{\psi}_A(0)\\
\hat{\theta}_B(t)&\approx(\omega_2-\tilde{\omega}_B(0))t+\phi_2+\tilde{\psi}_B(0)\\
&=\hat{\omega}_B(0)\,t+\phi_2+\tilde{\psi}_B(0)
\end{aligned}
\tag{13}
$$

for local stability characterization. Now, for the equilibrium under concern, let us consider $\hat{\omega}_A(0)=\omega_1$ and $\hat{\omega}_B(0)=\omega_2$ in (13). By using (12) and (13), the two-time scales averaged dynamics of the estimation errors can be written as

$$
\begin{aligned}
\dot{\overline{a}}_A(t)=&\lambda\Big\{-\overline{a}_A(t)+a_1\Big[\cos\big(\overline{\psi}_A(t)\big)-1\Big]-c_1\sin\big(\overline{\psi}_A(t)\big)\\
&-\mu_c\,\overline{a}_C(t)\Big\}\\
\dot{\overline{c}}_A(t)=&\lambda\Big\{-\overline{c}_A(t)+a_1\sin\big(\overline{\psi}_A(t)\big)+c_1\Big[\cos\big(\overline{\psi}_A(t)\big)-1\Big]\\
&-\mu_c\,\overline{c}_C(t)\Big\}\\
\dot{\overline{\psi}}_A(t)=&-\overline{\omega}_A(t)-\mu_\theta\dot{\overline{\delta}}_A(t)\\
\dot{\overline{\omega}}_A(t)=&\,\mu_\omega\dot{\overline{\delta}}_A(t)\\
\dot{\overline{a}}_B(t)=&\lambda\Big\{-\overline{a}_B(t)+a_2\Big[\cos\big(\overline{\psi}_B(t)\big)-1\Big]-c_2\sin\big(\overline{\psi}_B(t)\big)\Big\}\\
\dot{\overline{c}}_B(t)=&\lambda\Big\{-\overline{c}_B(t)+a_2\sin\big(\overline{\psi}_B(t)\big)+c_2\Big[\cos\big(\overline{\psi}_B(t)\big)-1\Big]\Big\}\\
\dot{\overline{\psi}}_B(t)=&-\overline{\omega}_B(t)-\mu_\theta\dot{\overline{\delta}}_B(t)\\
\dot{\overline{\omega}}_B(t)=&\,\mu_\omega\dot{\overline{\delta}}_B(t)
\end{aligned}
$$

and

$$
\begin{aligned}
\dot{\overline{a}}_C(t)&=-\lambda\,\overline{a}_C(t)\\
\dot{\overline{c}}_A(t)&=-\lambda\,\overline{c}_C(t)
\end{aligned}
$$

where we have used the notation

$$\begin{aligned}
\dot{\overline{\delta}}_A(t) &= \dot{\overline{\delta}}\left(\overline{a}_A(t), \overline{c}_A(t), \overline{\psi}_A(t)\right) \\
&= \frac{-\lambda}{(a_1+\overline{a}_A(t))^2+(c_1+\overline{c}_A(t))^2}\times \\
&\Big\{(\overline{c}_A(t)+c_1)\Big[-\overline{a}_A(t) - \mu_C a_C(t)+a_1\left(\cos\left(\overline{\psi}_A(t)\right)-1\right) \\
&\qquad -c_1\sin\left(\overline{\psi}_A(t)\right)\Big] \\
&-(\overline{a}_A(t)+a_1)\Big[-\overline{c}_A(t)- \mu_C c_C(t) +a_1\sin\left(\overline{\psi}_A(t)\right) \\
&\qquad +c_1\left(\cos\left(\overline{\psi}_A(t)\right)-1\right)\Big]\Big\} \\
&= \frac{-\lambda}{(a_1+\overline{a}_A(t))^2+(c_1+\overline{c}_A(t))^2}\times \\
&\Big\{-(a_1^2+c_1^2+\overline{a}_A(t)a_1+\overline{c}_A(t)c_1)\sin\left(\overline{\psi}_A(t)\right) \\
&+(\overline{a}_A(t)+a_1)(\overline{c}_A(t)-\mu_C\, a_C(t)) \\
&-(\overline{c}_A(t)+c_1)(\overline{a}_A(t)-\mu_C\, c_C(t)) \\
&+(\overline{c}_A(t)a_1-\overline{a}_A(t)c_1)\Big[\cos\left(\overline{\psi}_A(t)\right)-1\Big]\Big\}
\end{aligned}$$

and

$$\begin{aligned}
\dot{\overline{\delta}}_B(t) &= \dot{\overline{\delta}}\left(\overline{a}_B(t), \overline{c}_B(t), \overline{\psi}_B(t)\right) \\
&= \frac{-\lambda}{(a_2+\overline{a}_B(t))^2+(c_2+\overline{c}_B(t))^2}\times \\
&\Big\{-(a_2^2+c_2^2+\overline{a}_B(t)a_2+\overline{c}_B(t)c_2)\sin\left(\overline{\psi}_B(t)\right) \\
&+(\overline{a}_B(t)+a_2)\overline{c}_B(t)-(\overline{c}_B(t)+c_2)\overline{a}_B(t) \\
&+(\overline{c}_B(t)a_2-\overline{a}_B(t)c_2)\Big[\cos\left(\overline{\psi}_B(t)\right)-1\Big]\Big\}
\end{aligned}$$

Finally, to analyze the local stability of the equilibrium $(\Omega_{A,1,B,2})$ let us consider the linearized equations for small perturbations:

$$\begin{aligned}
\dot{\overline{a}}_A(t) &= \lambda\Big(-\overline{a}_A(t)-c_2\overline{\psi}_A(t) - \mu_C\overline{a}_C(t)\Big) \\
\dot{\overline{c}}_A(t) &= \lambda\Big(-\overline{c}_A(t)+ a_2\overline{\psi}_A(t)- \mu_C\overline{c}_C(t)\Big) \\
\dot{\overline{\psi}}_A(t) &= -\overline{\omega}_A(t) - \lambda\mu_\theta\overline{\psi}_A(t) \\
&\quad -\lambda\mu_\theta\left(-\frac{c_1}{a_1^2+c_1^2}\overline{a}_A(t)+\frac{a_1}{a_1^2+c_1^2}\overline{c}_A(t)\right) \\
&\quad -\lambda\mu_\theta\mu_C\left(-\frac{a_1}{a_1^2+c_1^2}\overline{a}_C(t)+\frac{c_1}{a_1^2+c_1^2}\overline{c}_C(t)\right) \\
\dot{\overline{\omega}}_A(t) &= \lambda\mu_\omega\left(-\frac{c_1}{a_1^2+c_1^2}\overline{a}_A(t)+\frac{a_1}{a_1^2+c_1^2}\overline{c}_A(t)+\overline{\psi}_A(t)\right) \\
&\quad +\lambda\mu_\omega\mu_C\left(-\frac{a_1}{a_1^2+c_1^2}\overline{a}_C(t)+\frac{c_1}{a_1^2+c_1^2}\overline{c}_C(t)\right)
\end{aligned}$$

$$\begin{aligned}
\dot{\overline{a}}_B(t) &= \lambda\Big(-\overline{a}_B(t)-c_2\overline{\psi}_B(t)\Big) \\
\dot{\overline{c}}_B(t) &= \lambda\Big(-\overline{c}_B(t)+ a_2\overline{\psi}_B(t)\Big) \\
\dot{\overline{\psi}}_B(t) &= -\overline{\omega}_B(t) - \lambda\mu_\theta\overline{\psi}_B(t) \\
&\quad -\lambda\mu_\theta\left(-\frac{c_2}{a_2^2+c_2^2}\overline{a}_B(t)+\frac{a_2}{a_2^2+c_2^2}\overline{c}_B(t)\right) \\
\dot{\overline{\omega}}_B(t) &= \lambda\mu_\omega\left(-\frac{c_2}{a_2^2+c_2^2}\overline{a}_B(t)+\frac{a_2}{a_2^2+c_2^2}\overline{c}_B(t)+\overline{\psi}_B(t)\right) \\
\dot{\overline{a}}_C(t) &= -\lambda\,\overline{a}_C(t) \\
\dot{\overline{c}}_C(t) &= -\lambda\,\overline{c}_C(t).
\end{aligned}$$

The dynamic matrix of the system for assigned a_1, c_1, a_2, c_2 is then given by the matrix $\mathbf{M}_{\Omega_{A,1,B,2}}$ shown in Figure III.

The local exponential stability of the estimate is guaranteed if the roots of the characteristic polynominal of $\mathbf{M}_{\Omega_{A,1,B,2}}$ have negative real parts. A sufficient condition for stability is therefore that λ, μ_θ and μ_ω are chosen such that the coefficients of the polynomial satisfy the usual Routh-Hurwitz conditions. The local exponential stability of the set $\Omega_{A,2,B,1}$ can also be established by proceeding along the same lines of the proof above.

IV. Example

The effectiveness of the proposed two-frequency detection approach is confirmed by the provided example, in which the following signal has been used to test the devised quadrature-based method:

$$v(t) = A_1\sin(\omega_1 t + \vartheta_1) + A_2\sin(\omega_3 t + \vartheta_2), \qquad (14)$$

with $\omega_1 = 2\pi 60$, $A_1 = 110$, $\vartheta_1 = 0$, $\omega_2 = 2\pi 61$, $A_2 = 12$, $\vartheta_2 = \pi/9$ for $t \in [0, 250)$. At time $t = 250$ the frequency and the amplitude of the second sinusoidal subsume a stepwise change: $\omega_2 = 2\pi 40$, $A_2 = 24$. The two filters FAF$_A$ and FAF$_A$ have been initialized with the same guessed frequency $\hat{\omega}_A(0) = \hat{\omega}_B(0) = 2\pi 60$ and with the following parameter set: $\hat{a}_A = 110$, $\hat{c}_A = 0$, $\hat{\theta}_A = 0$, $\hat{a}_B = 0$, $\hat{c}_B = 0$, $\hat{\theta}_B = 0$. The decorrelator has been initialized with $\hat{a}_C = \hat{c}_C = 0$, while the tuning parameters have been set to $\lambda = 0.1$ $\mu_\omega = 12$ $\mu_\theta = 1e{-}4$ and $\mu_C = 0.75$. The results of the simulation are shown in Figures 3 and 4, where the successful detection of the two sinusoidal components can be observed. Due to the perturbation introduced by the stepwise change on the frequency and amplitude of the second signal, the first sinusoidal term, detected previously by the FAF$_A$, is detected by FAF$_B$ after the transitory. The simulations have confirmed that changes from one stable configuration $(\Omega_{A,1,B,2})$ to the other $(\Omega_{B,1,A,2})$ may occur only due to sudden external perturbation, while the detection is not affected by beating phenomena after complete convergence.

Fig. 3 Estimated (solid-blu / FAF$_A$)-(dashed-green/ FAF$_B$) and true (dotted-back) time-evolution of fundamental frequencies for the two sinusoidal terms. The smaller-amplitude sinusoidal term changes stepwise its fundamental frequency ω_2 and amplitude A_2 at time instant $t = 250\,s$. After the frequency change, the estimator finds a new stable equilibrium.

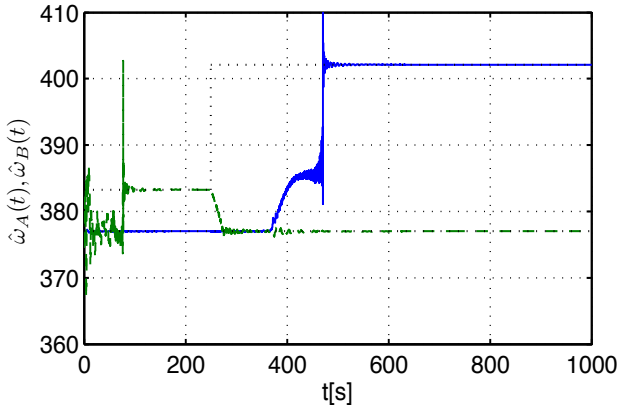

Fig. 2 Dynamic matrix of the error system (with respect to an arbitrary equilibrium in the set $\Omega_{A,1,B,2}$) linearized in the origin. The local stability can be achieved by a suitable choice of $\lambda, \mu_\theta, \mu_\omega, \mu_c$, for any value of the unknown parameters.

$$\mathbf{M}_{\Omega_{A,1,B,2}} = \begin{bmatrix}
-\lambda & 0 & -\lambda c_1 & 0 & 0 & 0 & 0 & 0 & -\lambda\mu_C & 0 \\
0 & -\lambda & \lambda a_1 & 0 & 0 & 0 & 0 & 0 & 0 & -\lambda\mu_C \\
\frac{\lambda\mu_\theta c_1}{a_1^2+c_1^2} & \frac{-\lambda\mu_\theta a_1}{a_1^2+c_1^2} & -\lambda\mu_\theta & -1 & 0 & 0 & 0 & 0 & \frac{-\lambda\mu_\theta\mu_C a_1}{a_1^2+c_1^2} & \frac{\lambda\mu_\theta\mu_C c_1}{a_1^2+c_1^2} \\
\frac{-\lambda\mu_\omega c_1}{a_1^2+c_1^2} & \frac{\lambda\mu_\omega a_1}{a_1^2+c_1^2} & \lambda\mu_\omega & 0 & 0 & 0 & 0 & 0 & \frac{-\lambda\mu_\omega\mu_C a_1}{a_1^2+c_1^2} & \frac{\lambda\mu_\omega\mu_C c_1}{a_1^2+c_1^2} \\
0 & 0 & 0 & 0 & -\lambda & 0 & -\lambda c_2 & 0 & 0 & 0 \\
0 & 0 & 0 & 0 & 0 & -\lambda & \lambda a_2 & 0 & 0 & 0 \\
0 & 0 & 0 & 0 & \frac{\lambda\mu_\theta c_2}{a_2^2+c_2^2} & \frac{-\lambda\mu_\theta a_2}{a_2^2+c_2^2} & -\lambda\mu_\theta & -1 & 0 & 0 \\
0 & 0 & 0 & 0 & \frac{-\lambda\mu_\theta c_2}{a_2^2+c_2^2} & \frac{\lambda\mu_\theta a_2}{a_2^2+c_2^2} & \lambda\mu_\omega & 0 & 0 & 0 \\
0 & 0 & 0 & 0 & 0 & 0 & 0 & 0 & -\lambda & 0 \\
0 & 0 & 0 & 0 & 0 & 0 & 0 & 0 & 0 & -\lambda
\end{bmatrix}$$

Fig. 4 Estimated(solid-blu / FAF_A)-(dashed-green/ FAF_B) and true (dotted-back) time-evolution of amplitudes for the two sinusoidal components.

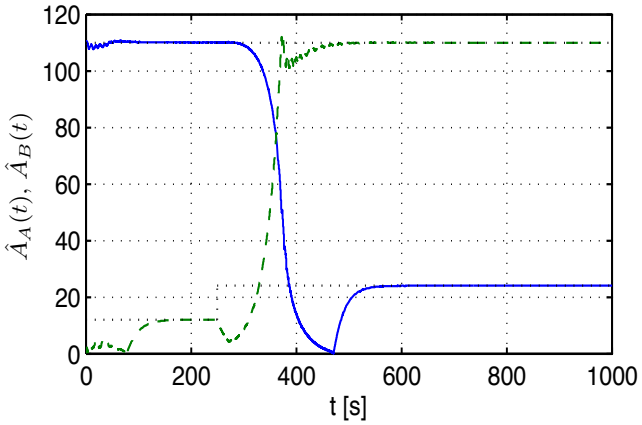

V. Conclusion

In the present work, a novel method for detecting the amplitude, the phase and the frequency of a couple of sinusoidal signals has been presented. The devised technique is based on the interconnection of quadrature-based frequency-adaptive filters. The stability properties of the scheme have been characterized by a two-time scale averaging analysis.

Further research will be devoted to address the frequency-detection in presence of a constant bias on the incoming signal and to extend the method to the generic N-frequencies case.

References

[1] J. Barbedo and A. Lopes, "Estimating frequency, amplitude and phase of two sinusoids with very close frequencies," *International Journal of Signal Processing*, vol. 5, no. 2, pp. 138–145, 2009.

[2] H. Li and P. Djuric, "A novel approach to detection of closely spaced sinusoids," *Signal Processing*, vol. 51, no. 2, pp. 93–104, 1996.

[3] P. Maragos, J.F.Kaiser, and T.F.Quatieri, "On amplitude and frequency demodulation using energy operators," *IEEE Trans. on Signal Processing*, vol. 41, pp. 1532–1550, 1993.

[4] B. Santhanam and P. Maragos, "Energy demodulation of two-component AM-FM signal mixtures," *IEEE Signal Processing Letters*, vol. 3, no. 11, pp. 294–298, 1996.

[5] S. Kim and Y.Park, "Active control of multi-tonal noise with reference generator based on on-line frequency estimator," *Journal of Sound and Vibration*, vol. 227, no. 3, pp. 647–666, 1999.

[6] M. Shahram and P. Milanfar, "Local detectors for high-resolution spectral analysis: Algorithms and performance," *Digital Signal Processing*, vol. 15, pp. 305–316, 2005.

[7] ——, "On the resolvability of sinusoids with nearby frequencies in the presence of noise," *IEEE Trans. on Signal Processing*, vol. 53, no. 7, pp. 2579–2588, 2005.

[8] P. O'Shea, "The use of sliding spectral windows for parameter estimation in power system disturbance monitoring," *IEEE Transactions on Power Systems*, vol. 15, pp. 1261–1267, 2000.

[9] ——, "A high-resolution spectral analysis algorithm for power-system disturbance monitoring," *IEEE Transactions on Power Systems*, vol. 17, no. 3, pp. 676–680, 2002.

[10] R. G. Brown, *Introduction to Random Signal Analysis and Kalman Filtering*. Wiley, 1983.

[11] B. Scala and R. Bitmead, "Design of an extended kalman filter frequency tracker," *IEEE Trans. on Signal Processing*, vol. 44, no. 3, pp. 739–742, 1996.

[12] S. Bittanti, M. Campi, and S. Savaresi, "Unbiased estimation of a sinusoid in colored noise via adapted notch filters," *Automatica*, vol. 33, no. 2, pp. 209–215, 1997.

[13] L. Hsu, R. Ortega, and G. Damm, "A globally convergent frequency estimator," *IEEE Trans. on Automatic Control*, vol. 44, no. 4, pp. 698–713, 1999.

[14] P. Regalia, "An improved lattice-based adaptive IIR notch filter," *IEEE Trans. on Signal Processing*, vol. 39, no. 9, pp. 2124–2128, 1991.

[15] S.-C. Pei and C.-C. Tseng, "Real time cascade adaptive notch filter scheme for sinusoidal parameter estimation," *Signal Processing*, vol. 39, no. 1-2, pp. 117–130, 1994.

[16] X. Guo and M. Bodson, "Frequency estimation and tracking of multiple sinusoidal components," in *Proc. of the IEEE Conf. on Decision and Control*, Maui, 2003, pp. 5360–5365.

[17] M. Karimi-Ghartemani, H. Karimi, and M. Iravani, "A magnitude/phase-locked loop system based on estimation of frequency and in-phase/quadrature-phase amplitudes," *IEEE Trans. on Industrial Electronics*, vol. 51, no. 2, pp. 511–517, 2004.

[18] G. Pin, "A direct approach for the frequency-adaptive feedforward cancellation of harmonic disturbances," *IEEE Trans. on Signal Processing*, vol. 58, no. 7, pp. 3513–3530, 2010.

[19] H. Khalil, *Nonlinear Systems*. Prentice Hall, 2001.

[20] J. Sanders and F. Verlust, *Averaging Methods in Nonlinear Dynamical Systems*. Springer-Verlag, 1985.

[21] S. Sastry and M. Bodson, *Adaptive Control: Stability, Convergence, and Robustness*. Prentice-Hall, 1994.